

Transient Thermal Elastohydrodynamic of Rough Surfaces under Line Contact with Non-Newtonian Solid-Liquid Lubricants

Chatchai Aiumpronsin¹ and Mongkol Mongkolwongrojn²

¹Mechatronics and Robotics Engineering Department, Faculty of Engineering, South-East Asia University, Bangkok, 10160.

²Mechanical Engineering Department, Faculty of Engineering, King Mongkut's Institute of Technology Ladkrabang, Bangkok, 10520

Abstract

The thermal compressible elastohydrodynamic lubrication of rough surfaces under line contact with non-Newtonian solid-liquid lubricants was investigated in transient operating conditions. Properties of non-Newtonian solid-liquid fluids have been obtained experimentally using solid particles namely, Molybdenum disulfide. The newly derived time-dependent modified Reynolds equation and the adiabatic energy equation have been formulated using a non-Newtonian power law viscosity model. The simultaneous systems consisting of the modified Reynolds equation, elasticity equation and energy equation with initial conditions were solved numerically using the multigrid multilevel method with a full approximation technique. The dynamic characteristics of the two infinitely long cylindrical rough surfaces in line contact under thermoelastohydrodynamic lubrication were presented with varying dimensionless time and with varying particle concentration for the pressure, temperature and oil film thickness profiles. The results of rough surfaces thermoelastohydrodynamic lubrication with non-Newtonian solid-liquid lubricants are compared with the case of smooth surfaces.

Keywords: Thermal elastohydrodynamic lubrication, Non-Newtonian solid liquid lubricants, Power law model, Modified Reynolds equation.

1. Introduction

When lubricated contacts in machine element applications are operated in severe conditions, the nominal film thickness in the contacts can be decreased to a level where surface roughness becomes significant. The lubricant film on the solid surfaces of the machine components become very thin. Therefore, the lubricant containing solid particles has greatly improved the lubrication characteristics in order to protect the contact surfaces. Many numerical solutions of elastohydrodynamic lubrication (EHL) for smooth surfaces and for rough surfaces problems were solved in the area ranging from transient elastohydrodynamic to thermal elastohydrodynamic using Newton-Raphson method and multigrid multilevel with full approximate scheme techniques [1-2]. In 1990, Khonsari, et al [3] showed that solid lubricant additives have significant effects in raising the film thickness, load capacity and friction coefficient in the full EHL regime. Mongkolwongrojn [4] investigated the transient thermoelastohydrodynamic lubrication with non-Newtonian liquid-solid lubricants in line contact with smooth surfaces under a sudden load change. The solid particles were found to have a significant effect on the TEHL characteristics. In 2010, Mongkolwongrojn [5] showed that the journal bearing with transverse surface roughness pattern in the bearing liner exhibit better stability.

In this research work, the integrated effect of moving surface roughness and sudden loading on pressure profile, film thickness profile and temperature profile is investigated numerically in a TEHL line contact with non-Newtonian liquid-solid lubricant using a power law model. Finite difference multi-grid multi-level with full approximation scheme techniques and Newton's method were implemented to examine the transient thermal elastohydrodynamic lubrication with non-Newtonian liquid-solid lubricants under the action of a sudden load change.

2. Governing Equations

2.1 Constitutive Equation

The governing modified Reynolds, elasticity, energy and load equilibrium equations were analyzed to obtain transient thermoelastohydrodynamic lubrication characteristics of two rough surfaces in line contact under a sudden load change. The relationship between shear stress and shear rate of the non-Newtonian lubricant in this work can be approximated using a power-law model as

$$\tau_{xy} = \mu^* (\partial u / \partial y) \quad (1)$$

where the equivalent viscosity is

$$\mu^* = m_0 \left[(\partial u / \partial y)^2 \right]^{\frac{n-1}{2}} \quad (2)$$

2.2 Modified Reynolds Equation

In this study, the flow can be approximated as a single-phase flow. Integrating the momentum and continuity equations, the time dependent modified Reynolds equation with non-Newtonian lubricant for infinitely long cylindrical roller can be obtained as.

$$\frac{\partial}{\partial X} \left[\bar{\rho} H^3 \left(\frac{1}{\bar{\mu}_{e2}} - \frac{\bar{\mu}_{e0}}{\bar{\mu}_{e1}^2} \right) \frac{\partial P}{\partial X} \right] = K \frac{\partial}{\partial X} (\bar{\rho} H) + K \frac{S}{2} \frac{\partial}{\partial X} \left[\bar{\rho} H \left(1 - 2 \frac{\bar{\mu}_{e0}}{\bar{\mu}_{e1}} \right) \right] + K \frac{\partial}{\partial t} (\bar{\rho} H) \quad (3)$$

where

$$K = \frac{\bar{u} \mu_0 R^2}{b^3 P_H} = \frac{\pi^2 U}{16 W^2}$$

$$\frac{1}{\bar{\mu}_{e,j}} = \int_0^1 \frac{Y^j}{\bar{\mu}^*} dY$$

The boundary conditions are

$$X = X_{inlet}; \quad P = 0 \quad \text{and} \quad X = X_{exit}, \quad P = \frac{dP}{dX} = 0 \quad (4)$$

The apparent viscosity in the power-law model needs to be included as a correction factor in the viscosity-temperature-pressure relationship; the correction factor needs to be modified for solid particles in the lubricant can be written as

$$\bar{\mu}^* = \frac{m_0}{\mu_0} \left| \frac{\bar{u}\pi}{8RWH} \right|^{n-1} \left| \frac{\partial u^*}{\partial Y} \right|^{n-1} \left\{ 1 + 2.5 \frac{\lambda \rho_0}{\lambda \rho_0 + (1-\lambda)\rho_p} \right\} \left\{ \exp \left((\ln \mu_0 + 9.67) \left[-1 + (1 + 5.1 \times 10^{-9} P_H P)^{0.5} \right] - \gamma T_0 (T^* - 1) \right) \right\} \quad (5)$$

The dimensionless density of the liquid–solid lubricant varying with pressure, temperature and mass concentration of particles can be written as

$$\bar{\rho} = \frac{\left[1 + \frac{0.6 \times 10^{-9} P_H P}{1 + 1.7 \times 10^{-9} P_H P} \right] \left[1 - \beta T_0 (T^* - 1) \right]}{1 - \lambda \left(1 - \frac{\rho_0}{\rho_p} \right)} \quad (6)$$

2.3 Elasticity Equation

The film thickness for an infinitely long line contact, including the deformation of the surfaces and harmonic roughness, is given as

$$H = H_0 + \frac{X^2}{2} - \frac{1}{\pi} \int_{X_{inlet}}^{X_{exit}} P(\xi) \ln |X - \xi| d\xi + A \left(\frac{R}{b^2} \right) \sin \left(\frac{2\pi}{l_\lambda} (bX - u_t) \right) \quad (7)$$

2.4 Energy Equation

The time-dependent energy equation in dimensionless form was formulated including the heat generated due to friction between the particles and surfaces. Therefore, the energy can be expressed as

$$\frac{\partial^2 T^*}{\partial Y^2} = K_{T1} \left(\frac{\partial H^2}{\partial p} \right) \left(\frac{\partial T^*}{\partial t^*} + u^* \frac{\partial T^*}{\partial X} \right) - K_{T2} \left(\frac{\bar{\mu}^*}{k_p} \right) \left[\frac{\partial u^*}{\partial Y} \right]^2 - K_{T3} \left(\frac{T^* H^2}{k_p} \right) \left(\frac{\partial P}{\partial t^*} + u^* \frac{\partial P}{\partial X} \right) - K_{T4} \left(\frac{H^2}{k_p} \right) \int_{X_{inlet}}^{X_{exit}} H dX \quad (8)$$

where

$$K_{T1} = \left(\frac{\bar{u} \rho_0 C_p b^3}{k_0 R^2} \right) \quad K_{T2} = \left(\frac{\mu_0 \bar{u}^2}{k_0 T_0} \right)$$

$$K_{T3} = \frac{\beta \bar{u} b^3 P_H}{k_0 R^2} \quad K_{T4} = \frac{f_p |\bar{u} S| E' b}{k_0 T_0}$$

The boundary conditions of the energy equation are

$$T_{1,i}^* = 1 + \frac{k_0 R}{\sqrt{\pi \rho_1 C_{p,1} k_1 b^3 \bar{u} \left(1 - \frac{S}{2} \right)}} \int_{X_m}^{X_i} \left(\frac{\bar{k}_{p,i}}{H_i} \right) \left(6T_{1,i}^* - 2T_{2,i}^* - 4T_{1,i}^* \right) \frac{dX'}{\sqrt{X_i - X'}} \quad (9)$$

$$T_{2,i}^* = 1 - \frac{k_0 R}{\sqrt{\pi \rho_2 C_{p,2} k_2 b^3 \bar{u} \left(1 + \frac{S}{2} \right)}} \int_{X_m}^{X_i} \left(\frac{\bar{k}_{p,i}}{H_i} \right) \left(4T_{2,i}^* - 6T_{1,i}^* + 2T_{1,i}^* \right) \frac{dX'}{\sqrt{X_i - X'}} \quad (10)$$

$$T^*(X=0) = 1 \quad (11)$$

The thermal model expressed by equation (8) to equation (10) are equivalent to those models.

2.5 Load Carrying Capacity

Spherical shaped MoS₂ particles are assumed to be uniformly distributed in the contact region and the particles undergo plastic deformation under the action of normal load. For a particle that deforms plastically when the mean contact pressure reaches the hardness of particle, H_d , the load carried by a plastically deformed particle can be written as

$$w_{p,i} = \frac{9}{16} \pi^3 H_d^3 \left(\frac{d_p}{E_{ps}} \right)^2 + p(x) \nu_p A_i \quad (12)$$

where A_i is the contact area of an individual particle due to plastic deformation and $w_{p,i}$ is the load supporting by an individual particle. Therefore, the load carrying capacity for all particles is

$$w_p = \sum_i^{N_z} \sum_i^{N_x} w_{p,i} \quad (13)$$

The total load carrying capacity of the mixture consists of two parts: one component results from plastic deformation of the particles, w_p , and the other component is due to hydrodynamic action, w_f . The dimensionless load balance equation can be written as

$$\int_{X_{inlet}}^{X_{exit}} P dX - \left(1 - \frac{W_p}{W} \right) \frac{\pi}{2} = 0 \quad (14)$$

During each time interval, the Reynolds, elasticity and energy equations are calculated using the boundary conditions and the initial conditions in Eq. (4), (9), (10) and (11) to obtain pressure and temperature distributions. The relative accuracy in pressure, mean temperature and hydrodynamic load are less than or equal to 0.0001. The input parameters used in the analysis are shown in Tables 1 and 2. The properties of the lubricant as shown in Table 1 were obtained experimentally. The Newtonian rheological model is used for pure SAE90 oil with the power law index of $n = 1$. The property values of MoS₂ particles is shown in Table 2

Table 1 Physical properties of the SAE 90 oil and roller material

Equivalent radius, m	0.05
Inlet temperature of lubricant, K	313
Viscosity of liquid, Pa.s	0.195
Inlet density of liquid, kg/m ³	892.8
Viscosity-Pressure index	0.5685
Viscosity-Temperature coefficient, K ⁻¹	0.05763
Coefficient of thermal expansivity, K ⁻¹	0.00074
Thermal conductivity of liquid, W/(m.K)	0.126
Specific heat of liquid, J/(kg.K)	1870
Equivalent modulus of elasticity of rolling/sliding, GPa	220
Poisson ratio of rolling/sliding	0.3
Wave length of roughness, (μm)	2.5

Table 2 Physical properties of solid lubricants, MoS₂.

Density, kg/m ³	4800
Brinell hardness, Pa	3.136×10 ⁹
Modulus of elasticity, GPa	34
Poisson ratio	0.13
Friction coefficient	0.1

3. Results and Discussion

The static and dynamic characteristics of TEHL line contact with non-Newtonian liquid-solid lubricants were determined under the sudden dimensionless load change from 3.0×10^{-5} to 1×10^{-4} and dimensionless speed parameter $U = 1 \times 10^{-11}$.

The effects of heavy load change were investigated for a surface with sinusoidal roughness of 0.05 μm amplitude using SAE 90 oil mixed with 20% MoS₂, 2 μm diameter, a load increase from 3.0×10^{-5} to 1×10^{-4} at dimensionless speed parameter $U = 1 \times 10^{-11}$ and slide/roll ratio $S = 0.1$. The wavelength of the sinusoidal surface roughness profile in transverse direction is kept fixed. The roughness induces sharp pressure ripples over the ridges and valleys of the roughness as shown in Fig.1. High fluctuating pressure amplitude near the leading edge contrasts with the fluctuating pressure amplitude near the trailing edge in the contact region. At $x = 0$, the pressure fluctuations vary from 0.36 GPa to 0.62 GPa under dimensionless load $W = 3.0 \times 10^{-5}$ at time $t = 0$ ms. After an application of the sudden heavy load from 3.0×10^{-5} to 1×10^{-4} , the fluctuating pressure increases and varies from 0.65 GPa to 1.75 GPa at time $t = 6$ ms. At the trailing edge, the pressure spike is very large, approximately equal to 2.7 GPa at time $t = 6$ ms, due to the significant effect on viscosity for a liquid-solid lubricant with rough surfaces.

The transient oil film thickness under sudden load change for sinusoidal surface roughness profile is shown in Fig. 2. After application of a step load change, the central film thickness at $x = 0$ mm increases from 1.40 μm at time $t = 0.0$ ms to 1.62 μm at time $t = 1$ ms but the minimum film thickness decreases from 1.11 μm at $t = 0.0$ ms to 0.99 μm. at $t = 1.0$ ms. Then the central film thickness at $x = 0$ mm decreases to 1.19 μm and the minimum film thickness decreases to 0.54 μm at time $t = 6$ ms. the film thickness increase at $x = 0$ mm in the early transient state is due to the interaction of pressure, temperature and viscosity. Fig. 3 shows the fluctuating mean temperature profile. The mean temperature at $x = 0$ mm varies from 40.6°C to 45.2°C at time $t = 0$ ms. The temperature then becomes very high after the step load increase and the mean temperature varies from 88.4°C to 181.5°C at time $t = 6$ ms. The maximum temperature becomes significantly high and is approximately equal to 297°C at time $t = 6$ ms.

For SAE 90 oil mixed with 20% MoS₂, 2 μm in diameter, and the surface with sinusoidal roughness of 0.05 μm amplitude, the fluctuating pressure profile, film thickness profile and mean temperature profile are compared with those for the smooth surface in a steady state as shown in Figs. 4-6 respectively. The maximum pressure at $x = 0$ mm is 1.75 GPa. The influence of roughness on the pressure profile is significant when compared with the pressure at $x = 0$ mm and the pressure spike for the smooth surface condition. For the smooth surface, the pressure at $x = 0$ mm and the pressure spike are equal to 0.87 GPa and 1.09 GPa respectively. Fig. 5 shows that the central film thickness at $x = 0$ mm for the surface with transversally oriented roughness is slightly thinner than the central film thickness for a smooth surface. The minimum film thickness for the rough surface at dimensionless load $W = 1.0 \times 10^{-4}$ and dimensionless speed

parameter $U = 1 \times 10^{-11}$ is equal to 0.63 μm and the minimum film thickness for smooth surface at the same operating condition is 0.80 μm at steady a state. At the leading edge, the fluctuating amplitude of mean temperature is very large when compared with the amplitude of the mean temperature at the trailing edge, as shown in Fig. 6.

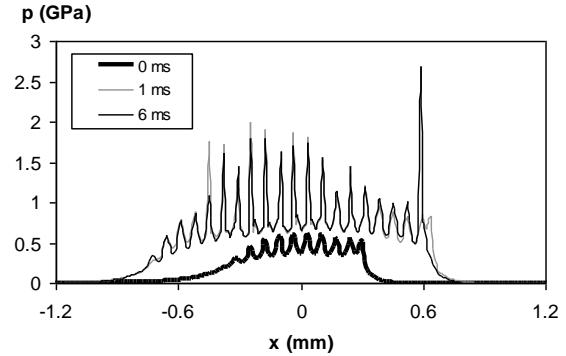


Fig. 1. Transient pressure profile under dimensionless load change from 3.0×10^{-5} to 1×10^{-4} , $A = 0.05$ μm

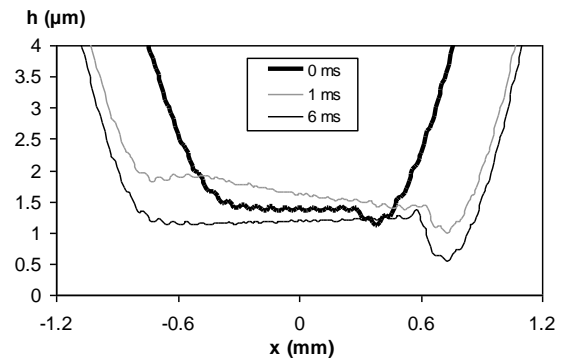


Fig. 2. Transient film thickness profile under dimensionless load change from 3.0×10^{-5} to 1×10^{-4} , $A = 0.05$ μm

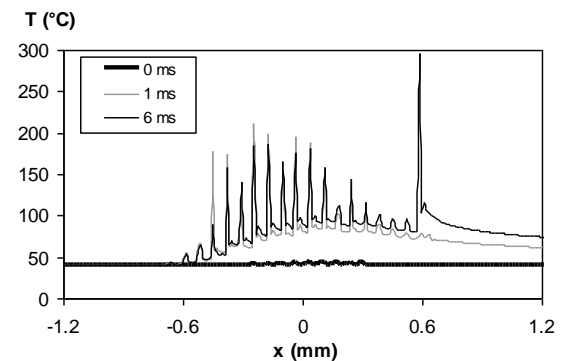


Fig. 3. Transient temperature profile under dimensionless load change from 3.0×10^{-5} to 1×10^{-4} , $A = 0.05$ μm

The largest mean temperature for the rough surface with 20% MoS₂ particles is equal to 188.3°C, compared with the largest mean temperature for a smooth surface, which is equal to 95.5°C as shown in Fig. 6.

Figs. 7-9 illustrate how the pressure, film thickness and mean temperature vary with increasing concentration of MoS₂ particles. With an increase in the concentration of MoS₂ particles, the maximum film pressure and maximum mean temperature and the minimum film thickness increase significantly for the rough surface. The maximum pressure,

minimum film thickness and maximum mean temperature are 1.80 GPa, 0.58 μm and 184.41 $^{\circ}\text{C}$ for SAE 90 oil without MoS_2 particle. The maximum pressure, minimum film thickness and maximum mean temperature for SAE 90 mixed with 30% MoS_2 particles are 1.84 GPa, 0.69 μm and 193.0 $^{\circ}\text{C}$ respectively. This increase in pressure is due to the increase in film temperature for the rough surface under the heavy load. Similarly, the average film pressure, film thickness and mean temperature at $x = 0$ mm for SAE 90 oil without MoS_2 particle at a steady state are 1.01 GPa, 1.04 μm and 113.5 $^{\circ}\text{C}$. The average film pressure, film thickness and mean temperature at $x = 0$ mm for SAE 90 oil mixed with 30% MoS_2 are 1.01 GPa, 1.16 μm and 114.5 $^{\circ}\text{C}$ respectively.

For the rough surfaces in line contact with 20% MoS_2 , the mean temperature is presented for different sizes of MoS_2 particles in Fig. 10. For MoS_2 particles with 2 μm diameter, the fluctuation of mean temperature is from 42.2 $^{\circ}\text{C}$ to 62.3 $^{\circ}\text{C}$, while for the 5 μm diameter particles, the fluctuation of mean temperature is from 42.6 $^{\circ}\text{C}$ to 65.6 $^{\circ}\text{C}$ for dimensionless load $W = 3.0 \times 10^{-5}$, $U = 1 \times 10^{-11}$. It is clear that for the larger particle sizes, the higher temperature is obtained, especially near the leading edge.

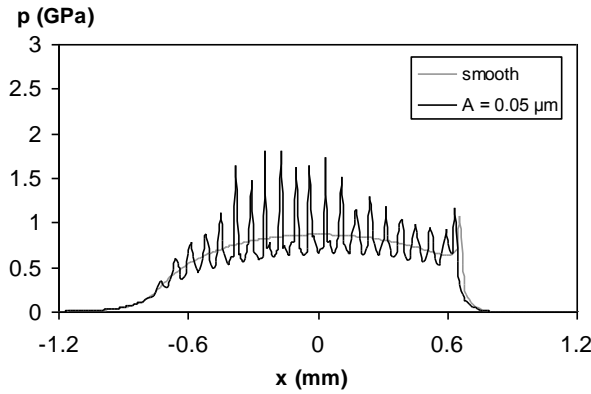


Fig. 4. Pressure profile under dimensionless load $W = 1 \times 10^{-4}$ at steady state

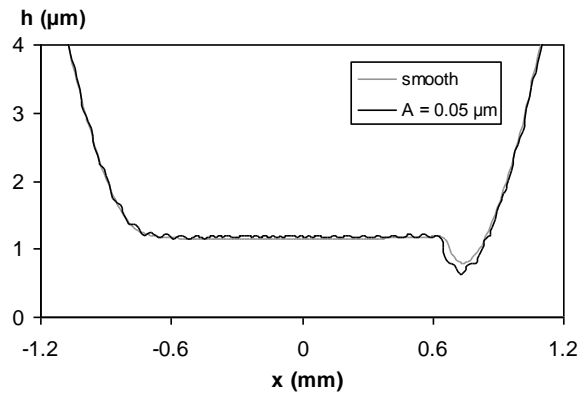


Fig. 5. Film thickness profile under dimensionless load $W = 1 \times 10^{-4}$ at steady state

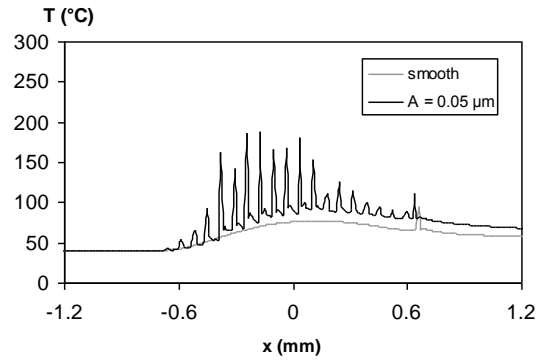


Fig. 6. Temperature profile under dimensionless load $W = 1 \times 10^{-4}$ at steady state

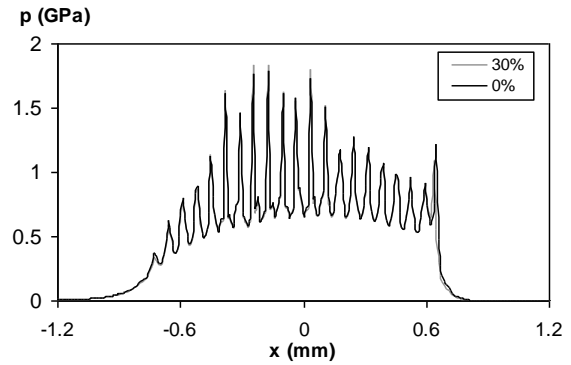


Fig. 7. Effect of particle concentration on pressure profile with 3 μm MoS_2 particles under dimensionless load $W = 1 \times 10^{-4}$, $A = 0.05 \mu\text{m}$

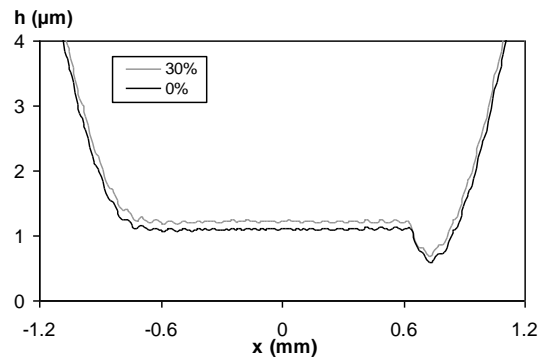


Fig. 8. Effect of particle concentration on film thickness profile with 2 μm MoS_2 particles under dimensionless load $W = 1 \times 10^{-4}$, $A = 0.05 \mu\text{m}$

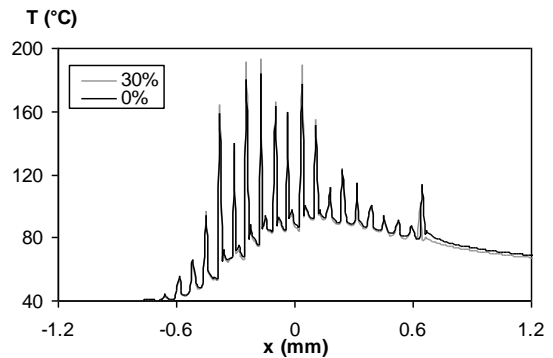


Fig. 9. Effect of particle concentration on temperature profile with 2 μm MoS_2 particle under dimensionless load $W = 1 \times 10^{-4}$, $A = 0.05 \mu\text{m}$

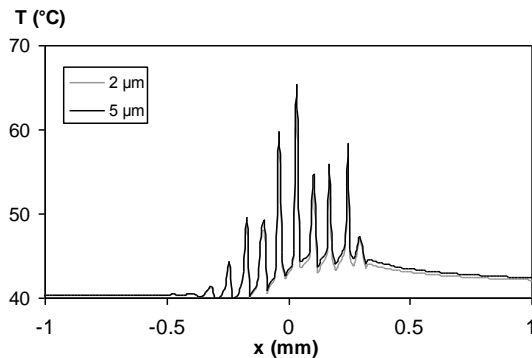


Fig. 10 Effect of particle size on temperature profile With 20% MoS_2 particles under dimensionless load $W = 3 \times 10^{-5}$, $A = 0.1 \mu\text{m}$

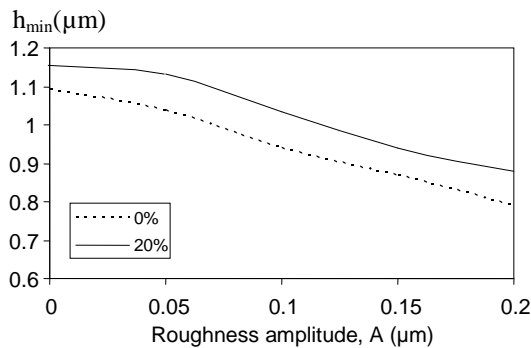


Fig. 11 Variation of minimum film thickness with the amplitude of roughness for $W = 3 \times 10^{-5}$, $U = 1 \times 10^{-11}$

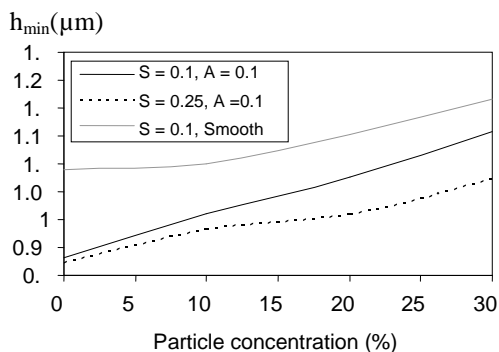


Fig. 12 Variation of minimum film thickness with concentration of MoS_2 particles for $W = 3 \times 10^{-5}$, $U = 1 \times 10^{-11}$

Fig. 11 shows the variation of minimum film thickness with the amplitude of surface roughness for 20% MoS_2 concentration at dimensionless load $W = 3.0 \times 10^{-5}$, $U = 1 \times 10^{-11}$ and $S = 0.1$. The minimum film thickness decreases nonlinearly with an increase in the amplitude of the surface roughness. One of the major reasons of adding MoS_2 additives to the liquid lubricant is to thicken them in order to increase the load carrying capacity of the oil film or to increase the minimum film thickness at a given load, the difference of the minimum film thickness for SAE90 oil mixed with 20% MoS_2 and for pure SAE90 is approximately $0.10 \mu\text{m}$. Fig. 12 illustrate the minimum film thickness increasing almost

linearly with an increase in MoS_2 concentration for smooth surfaces and for rough surfaces. The rate of the increase in minimum film thickness for rough surfaces is larger than the rate of the increase in minimum film thickness for smooth surfaces as shown in Fig. 12. It is clear that the minimum film thickness increases as the MoS_2 concentration increases. The minimum film thickness decreases with increasing the slip ratio for both the smooth and the rough surfaces. The effect of the slip ratio on the minimum film thickness for the higher concentration of solid particle is more significant than those for the low particle concentration.

4. Conclusions

The transient thermoelastohydrodynamic lubrication characteristics of a roller on flat surface in line contact with liquid-solid non-Newtonian fluids under a sudden load change was examined numerically. Analyses are performed for both smooth and rough surfaces. The main results presented can be summarized as:

- 1) Surface roughness induces high fluctuating pressure and fluctuating temperature. The maximum pressure and maximum temperature are significantly high for TEHL with liquid-solid lubricant.
- 2) The effects of roughness in the transverse direction on minimum film thickness are also significant. The minimum film thickness for rough surfaces is small when compared with minimum film thickness for smooth surfaces.
- 3) Surface roughness significantly increase the pressure and mean temperature in the lubricated contact when compared with those for smooth surface.
- 4) Large particles increase significantly the maximum temperature near the leading edge. This results in the reduction of viscosity and the lubricant film becomes very thin.
- 5) The oil film thickness increases rapidly due to surface roughness and the increase in pressure and oil viscosity in the early transient state after a sudden load increase, and then the oil film thickness decreases to the steady state equilibrium condition.
- 6) For rough surfaces, the average pressure and average temperature do not change significantly with variation in percent concentration of solid particles. This study shows that the solid particles can protect the lubricated contact in solid surfaces of machine or engine components.

5. Acknowledgments

This paper was partly supported from NASDA and College of Data Storage Technology KMITL.

6. References

- [1] Dowson, D., Higginson, G.R., 1959. Numerical Solution to lastohydrodynamic Problem. Journal of Mech. Eng. Sci, Vol. 1, pp. 6-15.
- [2] Ai, X., Chang, S.H., 1994. Transient EHL Analysis for Line Contacts with Measured Surface Roughness Using Multi-grid Technique. ASME Journal of Tribology, Vol. 116, pp. 549-558.
- [3] Khonsari, M.M., Wang, H.S., Qi, Y.L., 1990. A Theory of Thermo Elastohydrodynamic Lubrication of Liquid-Solid Lubricated Cylinders. ASME Journal of Tribology, Vol. 112, pp. 259-265.
- [4] Mongkolwongrojn, M., Aiumprorsin, C., Thammakosol, K., 2006. Theoretical Investigation in Thermoelastohydrodynamic Lubrication with Non-Newtonian Lubricants Under Sudden Load Change, Trans. Of the ASME Journal of Tribology, Vol.128, pp.771-777.
- [5] Mongkolwongrojn, M., Aiumprorsin, C., 2010. Stability Analysis of Rough Journal Bearings under TEHL with Non-Newtonian Lubricants. Tribology International, Vol. 43, pp. 1027-1034.

7. Nomenclature

- A = Roughness amplitude (m)
 A_i = Contact area of an individual particle
 b = Hertzian half-width (m), $b = R((8W)/\pi)^{0.5}$
 B = Width of rolling cylinders (m)
 E' = Equivalent modulus of elasticity (Pa)
 E_{ps} = Equivalent modulus of elasticity of particle and rolling/sliding (Pa)
 f_p = Friction coefficient of solid particle
 h = Film thickness (m)
 H = Dimensionless film thickness, $H = (R/b^2)h$
 H_d = Brinell hardness of particle (Pa)
 k_0 = Thermal conductivity of lubricant at ambient pressure (W/(m·K))
 \bar{k}_p = Dimensionless piezothermal conductivity
 l_λ = Wave length of roughness (m)
 m_0 = viscosity consistency (Pa·sⁿ)
 n = Power law index
 N_x = Number of particles in x-direction
 N_z = Number of particles in z-direction
 p = Pressure (Pa)
 P_H = Maximum Hertzian pressure (Pa), $P_H = E'(W/2\pi)^{0.5}$
 P = Dimensionless pressure, $P = p/P_H$
 R = Equivalent radius (m), $R = ((1/R_1) + (1/R_2))^{-1}$
 S = Slide ratio, $S = (u_2 - u_1)/\bar{u}$
 t = Time (s)
 t^* = Dimensionless time, $t^* = (\bar{u}/b)t$
 T = Temperature (K)
- T_o = Inlet temperature (K)
 T^* = Dimensionless film temperature
 u^* = Dimensionless velocity, $u^* = u/\bar{u}$
 \bar{u} = Mean velocity (m/s), $\bar{u} = (u_1 + u_2)/2$
 U = Dimensionless speed parameter, $U = (\mu_0\bar{u})/(E'R)$
 w = Applied Load (N/m)
 w_p = Load support by particle (N/m)
 W = Dimensionless load parameter, $W = w/(E'R^2)$
 W_p = Dimensionless load support by particle
 X, Y = Dimensionless coordinate $x = bX, Y = (R/b^2)(y/H)$
 z_l = Viscosity-Pressure index
- Greek**
- μ_o = viscosity at ambient pressure (Pa·s)
 μ^* = Equivalent viscosity (Pa·s)
 $\bar{\mu}^*$ = Dimensionless equivalent viscosity,
 $\bar{\mu}^* = \mu^*/\mu_o$
 ρ_o = Inlet density of oil (kg/m³)
 $\bar{\rho}$ = Dimensionless density, $\bar{\rho} = \rho/\rho_o$
 ρ_f = Density of oil (kg/m³)
 ρ_p = Density of particle (kg/m³)
 $\rho_{1/2}$ = Density of roller / slider (kg/m³)
 ν_p = Poisson ratio of particles
 ν_s = Poisson ratio of rolling/slider
 γ = Viscosity-Temperature coefficient (1/K)
 λ = concentration of particles by weight